39. V. B. Mountcastle, J. C. Lynch, A. P. Georgopoulos, H. Sakata, C. Acuna, *J. Neurophysiol.* **38**, 871 (1975); R. B. Muir and R. N. Lemon, *Brain Res.* **261**, 312 (1983); G. Rizzolatti *et al.*, *Exp. Brain Res.* **71**, 491 (1988); A. R. Mitz, M. Godschalk, S. P. Wise, *J. Neurosci.* **11**, 1855 (1991).
40. K. Okano and J. Tanji, *Exp. Brain Res.* **66**, 155 (1987); K. Kurata and S. P. Wise, *ibid.* **72**, 237 (1988).
41. V. B. Mountcastle, in *The Mindful Brain*, G. M. Edelman and V. B. Mountcastle, Eds. (MIT Press, Cambridge, MA, 1978), pp. 7–50; T. Iberall and M. A. Arbib, in *Vision and Action*, M. A. Goodale, Ed. (Ablex, Norwood, NJ, 1990), pp. 204–242.
42. Using tools, for instance, requires precise control of output forces (dynamics), whereas ballet demands precise control of limb motions (kinematics). Models that optimize just one performance criterion are too restrictive.
43. J. F. Kalaska, in *Brain and Space*, J. Paillard, Ed. (Oxford Univ. Press, Oxford, 1991), pp. 133–146.
44. A. Riehle, *Brain Res.* **540**, 131 (1991); P. Burbaud, C. Doegle, C. Gross, B. Bioulac, *J. Neurophysiol.* **66**, 429 (1991).
45. M. A. Arbib, in *Handbook of Physiology: The Nervous System*, V. B. Brooks, Ed. (American Physiological Society, Bethesda, MD, 1981), vol. 2, pp. 1449–1480; in *Attention and Performance XIII: Motor Representation and Control*, M. Jeannerod, Ed. (Erlbaum, Hillsdale, NJ, 1990), pp. 111–138.
46. G. E. Loeb, W. S. Levine, J. He, *Cold Spring Harbor Symp. Quant. Biol.* **55**, 791 (1991).
47. J. J. Hopfield, *Proc. Natl. Acad. Sci. U.S.A.* **79**, 2554 (1982); *ibid.* **81**, 3088 (1984); D. Rumelhart and J. McClelland, Eds., *Parallel Distributed Processing: Explorations in the Microstructure of Cognition* (MIT Press, Cambridge, MA, 1986).
48. T. J. Anastasio and D. A. Robinson, *Biol. Cybern.* **63**, 161 (1990); T. J. Anastasio, *ibid.* **64**, 187 (1991); D. B. Arnold and D. A. Robinson, *ibid.*, p. 447.
49. M. E. Nelson and J. M. Bower, *Trends Neurosci.* **13**, 403 (1990); E. I. Knudsen, S. du Lac, S. D. Esterly, *Annu. Rev. Neurosci.* **10**, 41 (1987).
50. M. Kawato, K. Furukawa, R. Suzuki, *Biol. Cybern.* **57**, 169 (1987); M. Kawato, M. Isobe, Y. Maeda, R. Suzuki, *ibid.* **59**, 161 (1988); L. Massone and E. Bizzi, *ibid.* **61**, 417 (1989); M. Brüwer and H. Cruse, *ibid.* **62**, 549 (1990); M. Kawato, Y. Maeda, Y. Uno, R. Suzuki, *ibid.*, p. 275; T. M. Martinetz, H. J. Ritter, K. J. Schulten, *IEEE Trans. Neural Netw.* **1**, 131 (1990); M. Kuperstein and J. Wang, *ibid.*, p. 137.
51. M. I. Jordan, in *Attention and Performance XIII: Motor Representation and Control*, M. Jeannerod, Ed. (Erlbaum, Hillsdale, NJ, 1990), pp. 796–836; H. C. Kwan, T. H. Yeap, B. C. Jiang, D. Borrett, *Can. J. Physiol. Pharmacol.* **68**, 126 (1988).
52. D. A. Robinson, *Behav. Brain Sci.*, in press; E. E. Fetz, *ibid.*, in press.
53. A. V. Lukashin, *Biol. Cybern.* **63**, 377 (1990).
54. R. A. Andersen, G. K. Essick, R. M. Siegel, *Science* **230**, 456 (1985); D. Zipser and R. A. Andersen, *Nature* **331**, 679 (1988).
55. Y. Burnod *et al.*, *J. Neurosci.*, in press.
56. E. E. Fetz and P. D. Cheney, *J. Neurophysiol.* **44**, 751 (1980); P. D. Cheney, E. E. Fetz, S. S. Palmer, *ibid.* **53**, 805 (1985); Y. Shinoda, J. I. Yokota, T. Futami, *Neurosci. Lett.* **23**, 7 (1981); E. J. Buys, R. N. Lemon, G. W. H. Mantel, R. B. Muir, *J. Physiol. (London)* **381**, 529 (1986).
57. B. W. Mel, *Connectionist Robot Motion Planning* (Academic Press, Boston, 1990).
58. A. Hein, *Brain Res.* **71**, 259 (1974); R. Held and J. A. Bauer, *ibid.*, p. 265; C. von Hofsten, in *Attention and Performance XIII: Motor Representation and Control*, M. Jeannerod, Ed. (Erlbaum, Hillsdale, NJ, 1990), pp. 739–762.
59. J. A. Adams, *J. Mot. Behav.* **3**, 111 (1971).
60. This learning has a proactive effect on subsequent movement; it is not moment-by-moment error correction.
61. H. C. Kwan, W. A. Mackay, J. T. Murphy, Y. C. Wong, *J. Neurophysiol.* **41**, 1120 (1978); K. C. Sato and J. Tanji, *ibid.* **62**, 959 (1989); D. R. Humphrey, *Fed. Proc.* **45**, 2687 (1986); R. N. Lemon, *Trends Neurosci.* **11**, 501 (1988); M. H. Schieber, *ibid.* **13**, 440 (1990).
62. H. C. Kwan, J. T. Murphy, Y. C. Wong, *Brain Res.* **400**, 259 (1987); G. W. Huntley and E. G. Jones, *J. Neurophysiol.* **66**, 390 (1991).
63. J. P. Donoghue, S. Suner, J. N. Sanes, *Exp. Brain Res.* **79**, 492 (1990); R. J. Nudo, W. M. Jenkins, M. M. Merzenich, *Somatosens. Mot. Res.* **7**, 463 (1990); K. M. Jacobs and J. P. Donoghue, *Science* **251**, 944 (1991).
64. A. Keller, A. Iriki, H. Asanuma, *J. Comp. Neurol.* **300**, 47 (1990).
65. D. J. Crammond and J. F. Kalaska, unpublished observations.
66. We thank G. Alexander, T. Drew, R. Dykes, E. Fetz, A. Georgopoulos, and D. Humphrey for useful comments. G. Filosi prepared Fig. 2. Supported by the Medical Research Council of Canada Group Grant in Neurological Sciences (J.F.K.) and a postdoctoral fellowship from Les Fonds de la Recherche en Santé du Québec (D.J.C.).

Physics of the Granular State

H. M. JAEGER AND SIDNEY R. NAGEL

Granular materials display a variety of behaviors that are in many ways different from those of other substances. They cannot be easily classified as either solids or liquids. This has prompted the generation of analogies between the physics found in a simple sandpile and that found in complicated microscopic systems, such as flux motion in superconductors or spin glasses. Recently, the unusual behavior of granular systems has led to a number of new theories and to a new era of experimentation on granular systems.

"To see a world in a grain of sand. . . ."
—*Auguries of Innocence,* WILLIAM BLAKE

SAND IN AN HOURGLASS, SALT PILES ALONG THE SIDE OF A highway, screes at the bottom of a mountain, and sugar in a bowl are all examples of familiar granular materials. These materials show a number of easily observed phenomena that are immediate manifestations of exceptional properties (Fig. 1). As distinct from liquids, granular heaps are stationary as long as the top surface is at a slope less than the "angle of repose," θ_r. No avalanches spontaneously occur until the slope is increased above the "maximum angle of stability," θ_m. When the slope is increased slightly above θ_m, grains begin to flow and an avalanche of particles occurs (Fig. 1B). However, instead of uniform motion throughout the sample, as expected in ordinary fluids, all of the motion occurs in a relatively thin boundary layer near the surface, which appears blurred. Between θ_r and θ_m is a region of complex, bistable behavior in which the material can be either stationary or flowing depending on how the pile was prepared.

There is also unusual behavior in a second simple configuration: a container filled with granular material up to a height, h. In a normal liquid, the pressure at the bottom of a filled vessel is proportional to the height of the liquid. In the case of granular material the pressure at the bottom of a sufficiently tall structure is independent of h because the friction of the particles along the wall of the container is sufficient to withstand the weight of the extra mass placed on its top. For this reason, in an hourglass filled with fine sand there is an approximately linear relation between filling height and draining time. Granular materials also show a phenomenon known as arching (or vaulting). In the building of a cathedral, the careful placement of a keystone at the top of an arch enables the creation of a vast empty space. Likewise, in a random configuration of grains, there will be places where arches appear naturally, leaving empty regions below. Granular material is inherently inhomogeneous, and the force network providing the stability of the system is nonuniform.

We have long been accustomed to divide matter into gases, liquids, and solids. Granular materials cut across these predefined boundaries. An example is the transition from solid- to liquid-like

The authors are with the James Franck Institute and the Department of Physics, The University of Chicago, Chicago, IL 60637.

behavior in Fig. 1. Sometimes granular materials behave in a manner different from that observed in all of the other classifications. Consider: sound propagates without much distortion in a gas; sound propagates equally well in a liquid and a solid. Even though individual sand grains are solid, the propagation of sound in granular materials is qualitatively different.

Many industries, such as the pharmaceuticals industry, depend on the processing of powders; the construction of highways, levees, and dams depends on the manipulation of large amounts of gravel and sand; bulk commodities from flour and grain to coal are transported, processed, and stored. Central to the design of the equipment for handling these materials are the flow and equilibrium properties of granular matter. In order to provide vibration isolation or shock absorption, structures often are embedded in containers filled with sand. In addition, a number of geological processes such as landslides, snow avalanches, and, to some extent, plate tectonics fit within the framework of granular materials.

Sandpiles have served as a macroscopic metaphor for thinking about many microscopic systems that are marginally stable. Analogies have been made to the motion of flux lattices in a superconductor and to relaxation in spin glasses; there are likely parallels to the physics of Josephson junction arrays and charge-density wave systems. In this way, the physics of granular materials touches a wide variety of phenomena that are still only partially understood. This article is not a comprehensive review of all aspects of granular materials, and we do not deal in detail with the area of rapid granular flow, which has been comprehensively reviewed (*1–3*). The unusual properties of these materials have also made this a subject of interest for science education (*4*).

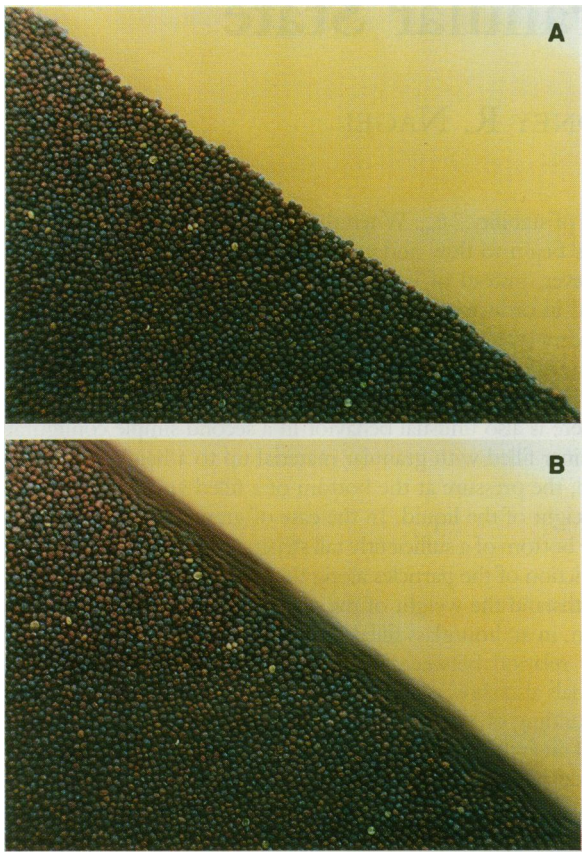

Fig. 1. A pile of mustard seeds (**A**) on the verge of and (**B**) during an avalanche. The pile was stable until the slope was increased above the maximum angle of stability. The finite-depth layer of seeds participating in the avalanche is the blurred region in the photograph.

An Unusual State of Matter

At first sight, the physics of a sandpile should be simple. Obviously, the masses of the individual particles are so large that classical mechanics is all that is relevant to their dynamics, and the thermal energy, k_BT, is unimportant (k_B, Boltzmann's constant; T, temperature). Also, the forces between the grains are often only repulsive, and there is negligible cohesion. Furthermore, the shape of the particles in many cases does not effect the qualitative behavior of the material, so they can be treated as point-like objects. Finally, a pile consists of many particles, so statistical methods should be applicable. What, then, makes the physics of these materials unusual?

It is tempting to think of each grain in a granular material as a large molecule in a normal gas or liquid. This approach has problems because it is immediately apparent that the particles are not moving, except due to global flow patterns, and the "temperature" to be used in such a "gas" would be 0 K. Thermal motion at finite temperatures allows many simplifications in our theories of matter. It allows an efficient way of averaging over many different configurations so that one does not have to treat each configuration separately. It is then possible to treat such a system as ergodic and to take ensemble averages. Without this constant averaging, a sandpile is an inhomogeneous material where the mechanical properties vary greatly from one point to the next. One example is the occurrence of arching. Arching cannot occur in a liquid or gas, where the continuous motion of the particles does not allow static configurations to form over any appreciable time period. The distribution of forces within a granular material will thus be modified by the existence of these arches in a way that the average properties of a liquid or gas will not.

Thermal motion allows a separation of scales in the problem. In normal liquids there is both a random thermal velocity as well as a drift velocity of the particles. The latter produces the coherent flow patterns in the system. In granular materials there is only the drift velocity; any random motion is generated by the drift velocity itself. Collisions in a flowing pile will occur on a time scale dictated by the flow rate and not, as in a normal liquid, at a rate determined by the mean free path and thermal velocity. This leads to different laws for the dissipation of energy in sheared systems. In a granular material, the mean free path for motion is comparable to, and often smaller than, the interparticle spacing. This corresponds to the strong-scattering regime in conventional systems.

Granular flow does not occur in a Newtonian fashion, as shown by the existence of a boundary layer in Fig. 1B. A natural approach might be to treat time-dependent phenomena in granular materials on the basis of a continuum fluid mechanics description, in analogy with the Navier-Stokes equations for hydrodynamics. However, it has been shown that such a procedure is fraught with difficulties and leads to instabilities in the equations. The implementation of such an approach is thus more difficult than it is even for normal liquids.

Geometry and Packing

The rigidity and flow characteristics of a granular material are determined by the geometrical packing of its constituent particles. In general the grains will form a disordered structure so that the properties of random packings become important. This subject goes back to Bernal (*5*) and Scott (*6*), who, using containers filled with steel ball bearings, studied random close-packed hard spheres in an attempt to model the molecular arrangements in simple liquids and glasses. Computer simulations by Finney (*7*) have confirmed that the maximum packing density (volume fraction of spheres) is $\eta \approx 0.64$ in the random close-packed (RCP) limit. It has long been assumed, but

without proof, that the densest possible packing in three dimensions is the close-packed hexagonal structure, which has $\eta \approx 0.74$. As the packing density is reduced, the continuous network of force-transmitting grain contacts becomes more tenuous and eventually breaks up. The point corresponding to the loosest random packing that is still mechanically stable under a given applied force, F, has been termed the random loose-packed (RLP) limit.

Of particular interest for sandpiles is the case where F is due only to the self-weight of the grains and is thus proportional to the gravitational acceleration, g. Recently Onoda and Liniger (*8*) investigated the limit of vanishing g, that is, the loosest possible random packing of mechanically connected grains, by immersing glass spheres in a liquid with variable specific density. They showed that the $g = 0$ limit for RLP corresponds to one continuous path of rigid connections throughout the array and occurs at $\eta = 0.56$. The entire variation from the most dense to a barely stable granular configuration therefore corresponds to an increase in average intergrain distance by a factor of only $(0.74/0.56)^{1/3} \approx 1.1$.

These results about the geometry of random-packed structures are relevant to the onset of flow in a granular material. As first described by Reynolds (*9*) in 1885, a granular material must expand in order to flow or deform at all. One can observe this dilatancy phenomenon when walking on a beach. The wet sand around one's foot dries out as weight is put on it. The deformation caused by the pressure of the foot causes the sand to expand and allows the water to drain away. Dilatancy arises from the need of a densely packed material to spread in order to make room for passing grains. The onset of dilatancy corresponds to the minimum packing density that requires expansion to allow internal shear. This, as for the $g = 0$ limit of RLP described above, occurs at $\eta \approx 0.56$.

Random close packing gives a framework with which to analyze the mechanical stability, the load-carrying capability, and the distribution of forces within a granular material under compression. Wakabayashi (*10*) and Ammi *et al.* (*11*) viewed the stresses in the individual particles of a two-dimensional pile by using polarized light and the photoelastic properties of the grains. Under an applied external pressure, a continuous network of connected bright spots appeared across the whole array, each spot corresponding to a stressed grain. This and related work (*12, 13*) clearly showed the existence of stress-transmitting paths enclosing virtually stress-free regions. Clearly, such stress-carrying networks must be important for determining the propagation of sound in these materials.

The distribution of forces in random networks is related to the rigidity threshold of the entire granular array (*14*). In general this is a nonlinear problem where the nonlinearity enters into the criterion for the occurrence of a local rupture. For example, if the force locally exceeds a threshold value, a grain may break or a permanent rearrangement may occur. In order to simulate this behavior, percolation models (*15*) based on nonlinear components such as diodes or fuses have been suggested (*14*).

Statistical Mechanics

As we argued in the introduction, thermal energy should be unimportant for the behavior of granular materials, so the concept of "temperature" should be otiose. Nevertheless, there are a number of contexts in which a generalized notion of temperature is important. When a granular material flows, there will be, in addition to an average velocity of the grains in the direction of the current, random velocities generated by collisions induced by the flow itself. The magnitude of the random velocity components will be approximately proportional to the average local shear rate. These random motions have been regarded (*16*) as a "granular temperature," in analogy with the thermal motion in molecular liquids and gases. In the presence of vibrations an analogous "effective temperature" may also be defined (*17*). In both of these situations the temperature is due to the random motion of the grains and is responsible for many observed phenomena such as particle diffusion, pressure, and the transport of momentum and energy (*3*).

The concept of granular temperature has not led to a full analogy with the statistical mechanics of molecular systems. Edwards and Mehta (*18, 19*) have recently proposed an alternative description of granular materials in complete analogy with statistical mechanics. In their formulation, the granular temperature does not appear.

Their basic assumption is that the volume V of a powder has the role played by the energy of a statistical system. Thus, instead of the Hamiltonian of the system, they introduce a function W, which specifies the volume of the system in terms of the positions of the individual grains. The "entropy" is, as usual, the logarithm of the number of configurations: $S = \lambda \ln[\int \delta(V - W) d(\text{all configurations})]$, where δ is the Dirac delta function and λ is the analog of Boltzmann's constant. Using this they are able to define a quantity, the "compactivity" X, which has the same role as temperature in statistical mechanics: $X = \partial V/\partial S$. In contrast to the notion of "granular temperature," which depends on the motions of the particles, the compactivity characterizes the static system. In the close-packed limit $X = 0$, and $X = \infty$ in the limit of low density.

Mehta and Edwards (*19, 20*) have applied their theory to the phase separation that occurs when a mixture of grains of two different sizes is vibrated. By mapping this problem onto the eight-vertex model (*21*) for a set of spins they were able to predict the occurrence of a phase transition as the compactivity is varied: for large values of X the mixing is totally random, whereas below a critical value, X_c, the system separates into two phases.

The segregation of mixtures of different-size particles by shaking is commonly observed and has important practical applications (*22*). For example, after transporting cereals one normally finds the larger flakes near the top of the box. In contrast to a liquid, where shaking generally will lead to a more homogeneous mixture, in the granular system the larger particles will rise to the top even for very small size differences or substantially denser large grains (*23, 24*). The result of the statistical theory discussed above indicates that for a given size difference there should be a critical value of the compactivity (or vibration intensity) where this segregation should begin.

Excitations

In general, if we want to know the underlying physics of a condensed matter system, we begin by studying its excitations. In the case of a granular material the excitations of interest clearly are the vibrations. At low amplitude, as with most other solids and liquids, vibrations constitute the sound waves; at larger amplitude they cause rearrangements in the structure of the material large enough to change the global shape of the sandpile. In both the large- and small-amplitude regimes, vibrations cause phenomena not normally observed in other types of materials.

Sound propagation. As the vibration intensity is decreased toward zero, one approaches the regime of ordinary sound propagation and attenuation. In a granular medium we find extraordinary behavior (*25*) because the properties of sound waves depend crucially on the compression of the contacts between the individual particles. If the particles are barely touching, there is only a very small restoring force to any movement of a grain. As the pressure, P, between grains increases there is greater deformation and a larger restoring force, and the velocity of sound increases (*26*). A model based on simple "Hertzian contacts" (*26–28*) suggests that the velocity, v, is propor-

tional to $P^{1/6}$. Far away from the container walls, where effects of friction with the wall can be neglected, the average pressure increases linearly with the depth, h, so that $v \propto h^{1/6}$, and the velocity goes to zero at the top of a pile. This implies the absence of horizontal sound propagation. If a plane wave is launched horizontally at any depth, it will not be able to sustain its horizontal motion. Its lower region will move faster so that the wave will gradually start to propagate with a vertical component. After a short distance it will be moving only in the vertical direction, creating a dramatic "mirage effect" (*25*).

The attenuation in a sound wave of a fixed frequency, ω, varies dramatically with time (*25*). The fluctuations in the signal can be as large as the average value of the signal itself. The frequency power spectrum of this noise reveals a power law, with an exponent of 2.2 over many orders of magnitude in frequency, f, extending down to $f = 10^{-5}$ Hz. This indicates correlations in the noise that last a full day. It is not yet understood why there is a power law (with a noninteger exponent), why the correlations last over such a long time, or how the noise depends on the amplitude of the source.

If one varies the frequency, ω, of the source, one finds that the response of the medium appears likewise to be "noisy." However, in this case it is reproducible over time. This behavior of the sound in a granular material is reminiscent of the electrical conductivity of small, mesoscopic, metal wires (*29, 30*). Over short length scales the conductivity of the wire is extraordinarily sensitive to the microscopic details. When any atom is moved or a field is changed, the conductance fluctuates by an average amount that is universal, independent of the magnitude of the conductance or of the source of the noise. The extreme sensitivity of the sound propagation in the sandpile is, in some sense, an analog to this behavior. What is new, however, is that the power spectrum for the noise has a rich and not understood behavior.

Vibrations and slope. Large-amplitude vibrations can modify the slope of a pile of sand. In the absence of vibrations a pile is stable with any slope smaller than θ_m, the maximum angle of stability. However, even at slopes below θ_m, vibrations allow the pile to relax. Although the prototypical relaxation of a nonequilibrium state back to equilibrium is exponential, the decay of the slope in sandpiles turns out to be logarithmic over several orders of magnitude in time (*17*).

We can derive this logarithmic decay if we assume that the vibrations mimic an effective temperature, T_{eff}, and that the particles move by "activated" hopping over barriers, of height U, created by their neighbors. The barriers decrease as the slope increases, and, because above θ_m the pile is unstable even when $T_{eff} = 0$, the barrier height must disappear at $\theta = \theta_m$. We thus approximate U with $U \cong U_1(\theta_m - \theta)$. By relating the particle flow, $j = d\theta/dt$, to the driving force, which is proportional to θ, we obtain

$$d\theta/dt = -A\theta e^{\beta(\theta-\theta_m)} \quad (1)$$

where $\beta = U_1/k_B T_{eff}$, A is a constant and t is time. For $\beta\theta \gg 1$ the solution to this equation is approximately

$$\theta = \theta_m - (1/\beta)\ln(\beta A\theta_m t + 1) \quad (2)$$

which fits the data well and is independent of the type of material used (*17*).

Logarithmic time dependence for relaxation has been observed in a variety of different systems, including the magnetization of spin glasses (*31*), amorphous ferromagnets (*32*), ferrofluids (*33*), high-temperature superconductors (*34*), and dipolar-coupled systems (*35*). The type of explanation used here for understanding the decay of the slope is useful in those cases as well. The nonexponential relaxation of the magnetization, $M(t,T) \propto (k_B T/U_1)\ln t$, is consistent with most of the data available on high-T_c superconductors (*36*) and is also known to apply to conventional type II superconductors (*37*). This form of the equation is characteristic for thermally activated flux creep, a process in which relaxation occurs by hopping of magnetic flux bundles over free energy barriers separating adjacent pinning sites, very similar (*38*) to how we modeled the motion of grains in the presence of vibrations.

Whereas the above discussion is based on a picture of diffusion along the surface of the pile, Duke *et al.* (*39*) have proposed a mechanism based on bulk relaxation to explain the data. In a Monte Carlo study of packings of polydisperse disks they simulate a vibration cycle by small random displacements of individual disks, followed by relaxation into a stable configuration. Starting with a loosely packed configuration they also found that the slope decreases with a logarithmic time dependence that covers several orders of magnitude. They related this dependence to the cumulative effect of small changes occurring in the network of contacts within the pile.

Pattern formation. For accelerations a where $a > g$ (g is the acceleration due to gravity) a different set of phenomena appears. Two groups, Evesque and Rajchenbach (*40*) and Fauve and coworkers (*41*), recently showed that in this regime the free surface of a pile of grains undergoes a convective instability: an initially flat, horizontal surface of material will spontaneously incline itself at a slope approaching the angle of repose, θ_r. Once a steady state is reached, transport of material down the slope is balanced by bulk convection of grains to the top of the pile. Faraday (*42*) first observed such convective motion in 1831. He emphasized the importance of the pore fluid, air, in his interpretation. Yet a full understanding of the underlying mechanism is still lacking. In fact, the recent experimental results have newly fueled a controversy over the importance of the interstitial fluid for convection. An underlying unresolved issue is the problem of how forces are transmitted from the vibration source, usually at the bottom of the heap, through the network of grain contacts to the surface of the pile, and the question of under what conditions the overall behavior can be separated into a collective, pistonlike motion of the bulk of the pile and an independent surface layer that appears fluidized.

Beyond $5g$ new instabilities arise. In thin layers of granular material, 10 to 100 particles high, Duady *et al.* (*43*) discovered that a period-doubling instability leads to the formation of spatially stationary patterns oscillating at half of the driving frequency. With increasing vibration intensity, a further transition to chaotic motion occurs with no stationary configurations, in either space or time.

Granular Flow

Modern studies of granular flow were pioneered by Bagnold (*44*), although early studies in this area were initiated by Hagen (*45*) in 1852 and Reynolds (*9*) in 1885. Most of the work has focused on one particular limit, namely fully developed, steady-state flow, which is of widespread importance for industrial applications. Until recently, time-dependent properties of granular flow had been almost completely unexplored. An extensive mathematical machinery for the description of steady-state flows based on the methods of continuum mechanics has been available. In addition, more recent refinements of this approach by Savage (*46*), Jenkins (*47*), Haff (*48*), and their collaborators have successfully introduced statistical tools from kinetic gas theory, and these researchers have considered models of the energy and stress distributions resulting from collisions in a dense gas of idealized spherical or disk-shaped particles. However, as these workers have pointed out (*46, 47*), important differences from the usual assumptions of classical kinetic gas theory exist: particle collisions will in general be inelastic. This means that the natural equilibrium state is a static configuration with granular temperature of absolute zero. Collisions and velocity fluctuations in a granular flow can only arise from gradients in the average flow

profile, which have to be provided by external sources of energy, such as shear forces. Much of the analytical work has been complemented by large-scale computer simulations (*3, 49, 50*), which allowed the direct evaluation of the stress tensor and flow profiles.

Rapid shear flows. There are two usual geometries that are considered in the study of rapid shear flows. For flow driven by gravity alone, inclined chutes and planes have been used (*51*). When, in addition, external forces are acting from one surface, annular shear cells (*52*) have been used in which two halves of an annulus filled with the granular material rotate against each other under a variable perpendicular loading force (*53*). If sidewall effects can be neglected, the steady-state properties depend only on the depth z into the flow. One aim of the work in this area has been the determination of the complicated velocity and density profiles as a function of inclination angle or loading force and shear rate. The shear rate $\dot{\gamma} \equiv \langle dv/dz \rangle$, that is, the average velocity gradient of the flow, enters because it is the relative velocity of grains that provides the mechanism for friction. In the simplest model, from Bagnold (*44*), a smooth velocity profile is assumed. The kinetic energy dissipated through collisions between grains of diameter D, mass m, and average relative velocity $D\dot{\gamma}$ in the x direction then leads to an average friction force

$$F_k = \left\langle \frac{dE_{kin}}{dx} \right\rangle = \frac{mD^2}{2\lambda_e} \dot{\gamma}^2 \qquad (3)$$

where λ_e, the mean distance for the dissipation of any excess energy, depends on the packing density of grains and will typically be one to several times the grain diameter D.

When there is an interstitial fluid between the grains the different types of flow can be characterized by the Bagnold number (*44*), which gives the ratio of intergrain-collision forces F_k to viscous forces $\mu\dot{\gamma}$: $B = mD^2\dot{\gamma}/2\lambda_e\mu$. Here μ is the interstitial fluid viscosity. Flows with $B < 40$ are called macro-viscous because the viscous interaction with the pore fluid is important. For $B > 450$ the flow is considered to be in the grain-inertia regime where grain-grain collisions dominate. Examples of macro-viscous flow are mud slides, debris flow (*54*), and transport of saturated sand-water mixtures in river beds (*55*). All flows with air as the interstitial fluid typically have B of order 100,000.

For high shear rates the quadratic Bagnold friction force law, Eq. 3, is well supported by shear-cell experiments (*52*). The opposite limit, associated with instabilities and the onset of flow, has been left largely unexplored. These are precisely the aspects that have made granular materials a model system from a physicist's perspective.

Instabilities in flow through apertures. More complicated behavior leading to pattern formation and dynamic instabilities occurs in granular flow through an aperture, a geometry of particular relevance to many industrial applications. The pressure, and therefore the flow rate, at the bottom of a column of granular material is independent of its height (*56*). However, the flux of grains leaving a container through an aperture produces complex flow regions inside the container. Brown and Hawksley (*57*) identified four distinct regions of density and velocity, most notably a "tongue" of intense motion just above the aperture, and an area of no grain motion below a cone extending upwards from the opening. To visualize the flow patterns, dyed grains (*58*) as well as x-ray techniques (*59, 60*) have been used. Baxter *et al.* (*60*) showed that for large opening angles ϕ, density waves propagate upward from above the aperture against the direction of particle flow, but downwards for ϕ less than 35° (Fig. 2). In mixtures of smooth and rough sand a proportion of at least 25% of rough, faceted grains are necessary in order to observe this phenomenon.

Schaeffer and Pitman (*61*) analyzed the flow in a hopper using

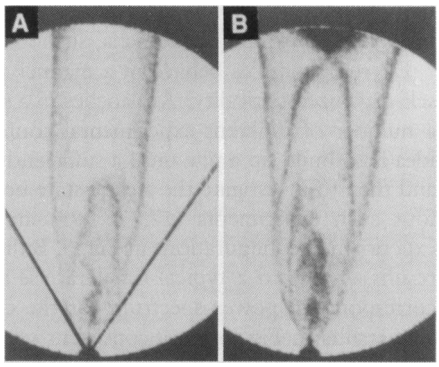

Fig. 2. Digital subtraction x-ray images of rough sand in a hopper (**A**) 12 s and (**B**) 15 s after the flow started. The dark patterns correspond to low-density fronts that propagate through the hopper. The field of view is a 10-inch circle. The sidewalls of the hopper are not visible because of the subtraction technique, but are indicated by the black lines in (A). Adapted from (*60*).

Navier-Stokes–type equations derived from plasticity theory and derived the existence of flow instabilities and propagating density waves. They approximated the material in the hopper by a uniform medium and analyzed Navier-Stokes–type equations derived from plasticity theory (*62, 63*). This approach treats the medium as uniform and ignores granularity. Alternative explanations (*60*) rely explicitly on the granularity: grains can interlock and form load-supporting arches with less densely packed material underneath. Because faceted grains are more likely to interlock than smooth ones, it is plausible that a minimum fraction of rough material is required to bridge the flow region and start a propagating front.

If the flowing particles have a nonspherical shape, their orientations are affected by the flow. The long axis of prolate ellipsoids will point along the direction of motion. This was observed in the flow of grass seed through a hopper by Baxter and Behringer (*64*) (Fig. 3, A through C). Results from the same authors of a cellular automaton model simulating this process are shown in Fig. 3, D through G. By including an interaction between the velocity and the orientation of a particle they succeed in reproducing many of the qualitative features of the flow. It is remarkable that such a simple model can reproduce the results of what is inherently a very complicated experimental situation.

Avalanches and self-organized criticality. Consider again the sandpile. It is appealing to think of a generalized phase transition occurring at θ_r: for $\theta < \theta_r$ the pile is stable and no flow occurs, whereas for $\theta > \theta_r$ flow can occur. To understand such an analogy one needs to examine what happens close to θ_r. Recently Bak, Tang, and Wiesenfeld (*65*) introduced the concept of "self-organized criticality," in which the critical state is an attractor for the dynamics of the system, using the avalanches in sandpiles as the generic illustrative example. They argued that the nonequilibrium state of the pile at θ_r would be a critical state in the sense of a second-order phase transition. A slight increase in θ would lead to avalanches characterized by both long-range spatial and temporal correlations. Self-organization would imply that the pile automatically drives itself to a critical state without the need to adjust any parameters externally. As a consequence of the underlying correlations they predicted scaling behavior for quantities such as avalanche sizes and frequency of occurrence. These scaling properties subsequently have been investigated (*65–69*) for a number of cellular automata sandpile models. Such automata form the basic model for self-organized criticality. Figure 4 shows the simple rules governing a typical cellular automaton for avalanche dynamics (*69*). In general, these models exhibit behavior more complicated than that found in conventional critical phenomena. For example, in one-dimensional models (*69*), multifractal analysis (*70*) must be used rather than a simple finite-size scaling analysis. However, although the scaling behavior may be more complicated in these nonequilibrium systems

than what one expects at equilibrium phase transitions, some properties of critical phenomena, such as universality, persist.

Do real sandpiles behave in a manner predicted by the ideas of self-organized criticality? Avalanches in a sandpile can be studied in a number of different experimental configurations. The principal idea is to build up a pile until a sufficiently steep slope θ is reached and then to investigate the steady-state behavior (*71*). Diagrams of four such experiments (*17, 72, 73*) are shown in Fig. 5. The experimental configurations in Fig. 5, B through D, produce similar results. In Fig. 6 a typical time trace is shown together with the corresponding power spectrum for the configuration in Fig. 5C. The results in Fig. 6 are inconsistent with the present concept of self-organized criticality, which, for the power spectrum, predicts a power law behavior, $f^{-\alpha}$. Originally the model calculations by Bak, Tang, and Wiesenfeld (*65*) gave $\alpha \cong 1$ [thus the connection to the widespread phenomenon of "1/*f*" noise (*74*)]. In real granular material we find that the power spectrum is indicative of a linear superposition of global, system-spanning avalanches with a narrowly peaked distribution of time scales. In addition, there is hysteresis $\delta = \theta_m - \theta_r$ that is not included in the model calculations. This hysteresis can be reduced to zero by low-intensity vibrations, which, however, do not bring the system towards criticality (*17*).

The experiments suggest that the behavior of sandpiles is self-organized but not critical. The mechanism for initiating an avalanche is more akin to a nucleation and growth phenomenon than to critical fluctuations, and the data resemble more what one would expect from a first-order phase transition. Real sandpile avalanches thus display dynamics that appear to belong to a larger class of self-organized behavior, which would include both critical and noncritical systems. But might it be possible to move between these two types? There is no clear answer to this intriguing question, although there are a few hints. Any motion of real grains down the slope involves a balance of gravitational forces connected with the grain inertia and friction forces resulting from dissipation. In the models and simulations a completely overdamped situation typically is assumed; that is, the friction term far outweighs the inertia term. The observed hysteresis indicates that the experiments might instead be in a regime where those two terms are of comparable magnitude. The situation can be altered by immersing the sand in a buoyant fluid or by increasing other sources of dissipation, such as friction with the walls, in relation to the normal grain-grain collisions. Indeed, as the width of a drum (Fig. 5) is decreased to about 5 to 10 grain diameters, the distribution of avalanche durations broadens considerably (*75, 76*). A complementary approach has been suggested by Evesque (*77*): this approach uses the variation of effective gravity (for example, by placing the system in a centrifuge) in order to change from first- to second-order behavior.

Held *et al.* studied the case in which individual grains were added one at a time to the apex of an extremely small pile (Fig. 5A) (*72*). If the radius of the base of the pile was less than approximately 30 bead diameters, the distribution of avalanche sizes appeared broad, resembling the scaling behavior predicted by the model of self-organized criticality. However, it has been argued that finite-size effects dominate the behavior in this regime (*75*). This argument would suggest that the behavior in the small-size regime is not representative of dynamics at a critical point. Rather, the fluctuations that occur appear to be due simply to the system being too small for it to show the two distinct angles θ_r and θ_m that determine the behavior in the infinite system.

Friction in sand. In order to explain some of the phenomena mentioned above one can set up a simple friction law for the motion of a grain of sand within a pile (*78*). If one starts with Newton's laws,

$$ma = mg\sin\theta - F \quad (4)$$

where F is the friction force retarding the motion and a is the acceleration. A steady state corresponds to $a = 0$ so that the friction

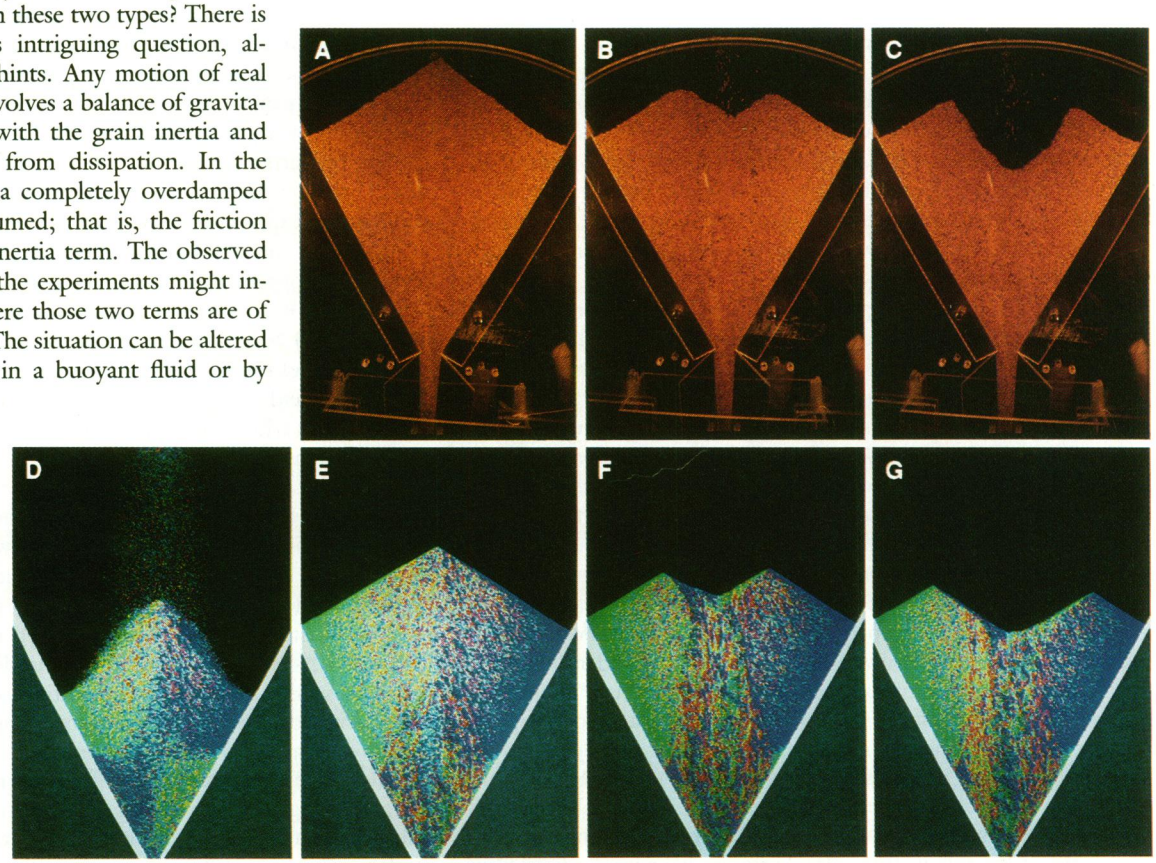

Fig. 3. Photographs of grass seed flowing through a hopper (**A**) immediately, (**B**) 0.6 s, and (**C**) 2.6 s after the opening of the aperture. The grass seeds rapidly align along the direction of the flow. (**D** through **G**) Cellular automata simulations on a triangular lattice of the same process. For each site a velocity and orientation is assigned. The particle can either be at rest or can move with velocity $\pm|v|$ along any of the three lattice directions. The orientation can likewise be along any of the three lattice directions. The colors indicate the orientation of the "seeds" (blue, inclined to the left; green, inclined to the right; red, vertical). The images show (D) the filling process, in which particles are added from the top with random orientations (the "crosslike" green and blue background pattern in the hopper is caused during the early stages of the filling process, where the grain orientations are influenced by the hopper walls); (E) the initial stages of flow, during which a pulse propagates to the top of the hopper, leading to the reorientation of many grains along the vertical (red) direction; and (F and G) fully developed flow. The top surface of the pile shows a shape similar to that of the experiment. Adapted from (*64*).

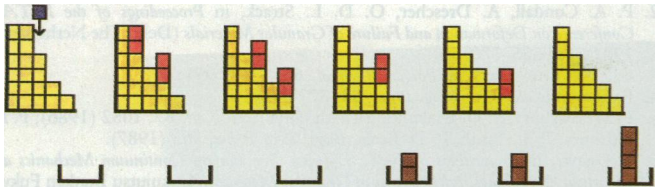

Fig. 4. Example of an "avalanche" in a one-dimensional cellular automaton model. The height of the "pile" along the horizontal axis is given by the number of particles stacked at each position. Initially, the "pile" is stable. Then the blue particle is added to a random position. The local slope, that is, height difference, at that point becomes larger than a critical value (in this model two units greater than the height of its neighbor), and two particles move to the right. This leaves the four red particles unstable, and the avalanche continues until a total of four particles have fallen off the right edge.

force just balances the driving force: $F = mg\sin\theta$. One can calculate the friction from $F = dE/dx$, where E is the energy of the particle and x is the distance traveled in the forward direction. There will be two contributions to E. The first will be the kinetic energy (relative to the layer on which the particle is moving) $E_k = m(D\dot{\gamma})^2/2$, which leads to F_k, the term given in Eq. 3, which was derived by Bagnold. There will also be a contribution from the potential energy $E_p = mg_\perp h$, where h is the height of the particle and $g_\perp = g\cos\theta$. The particle will lose its kinetic energy because of collisions in the close-packed system and its potential energy because of falling into depressions between particles in the layer on which it is moving (Fig. 7). These two sources of dissipation lead to a friction law

$$F = mg\left[\frac{a_1}{1 + b_1\left(\frac{D\dot{\gamma}^2}{g}\right)} + c_1\left(\frac{D\dot{\gamma}^2}{g}\right)\right] \quad (5)$$

where a_1, b_1, and c_1 are dimensionless constants.

At zero velocity, Eq. 5 has a finite value corresponding to Coulomb friction (*79*). The force F decreases as the velocity increases until it reaches its minimum value, after which it starts to increase rapidly. In a sandpile the maximum value of F at $\dot{\gamma} = 0$ corresponds to $mg\sin\theta_m$, its value just before the pile becomes unstable. Above this value the grains must move. The value of the friction at its minimum value is $mg\sin\theta_r$. Below this value, the only steady-state solution for the pile is to be stationary. Although between θ_m and θ_r there are three steady-state solutions, the middle one, in which the slope of F versus $\dot{\gamma}$ is negative, is unstable. The two others, at $\dot{\gamma} = 0$ and at large velocity, are both stable. In this region there is hysteresis because, depending on the initial conditions of the system, the pile may be in one or the other of the two stable solutions. This corresponds to stick-slip behavior. Whenever avalanche flow occurs it does so in a non-Newtonian manner: the flowing region is confined to a finite boundary layer and does not penetrate into the bulk of the material (Fig. 1). This phenomenon is also found in slow shearing experiments, where the failure zone is typically of the order of 10 grains thick (*80*). Because the minimum in the $F(\dot{\gamma})$ curve occurs at a finite value, this form of a friction law can account for the existence of a boundary layer in the flowing material.

Thompson and Grest (*81*) recently performed a molecular dynamics simulation of a two-dimensional sandpile in order to investigate the nature of the frictional forces. They concluded that there was indeed an unstable region below some critical value of the shear rate in agreement with the model of friction presented above. Above this value of $\dot{\gamma}$ the friction force increased with increasing shear rate, leading to stable slipping. Below this value, however, they found that the material exhibited nonuniform motion and stick-slip behavior, which they interpreted as being due to dilatancy transitions. In this regime a smooth friction curve could not be determined because of the instability inherent to the system.

Equation 5 has an electronic analog. Threshold angles such as θ_m or θ_r correspond to applied voltages or currents beyond which the electronic system becomes unstable. The motion of grains down the slope of a sandpile bears close resemblance to the motion of a particle in a tilted washboard potential. In the case of Josephson junctions or charge-density waves the corrugation minima correspond to stable positions for the system dynamics. The driving force $mg\sin\theta$ derived from the tilt of the pile might be thought of as an applied bias current I in the Josephson junction. If I becomes too large, the minima in the washboard potential disappear and trapping no longer occurs. This implies a switch from a state of zero voltage across the junction to a state of finite voltage V,

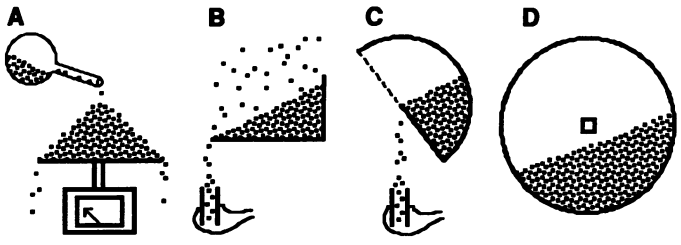

Fig. 5. Diagrams of four geometries for studying the dynamics of avalanches. (**A**) Grains are added one by one to the top of a pile, which forms on the flat, round platform of a sensitive digital scale interfaced to a computer (*72*). Excess grains fall off the platform and the scale measures the total weight at a given instant. (**B** and **C**) Changes in the slope are obtained by either randomly sprinkling sand onto the top surface of a pile confined by three walls and with one open side (B) (*17*) or rotating a semicylindrical drum at a very slow rate (C) (*17*). In both cases grains falling off the pile are detected by a capacitor underneath the platform's edge. Capacitance changes correspond directly to changes in the flow of particles, and resolution is sufficient to detect the passage of a single particle. The time sequence of capacitance changes, ΔC, is fed into a spectrum analyzer to obtain its power spectrum. (**D**) Avalanches are detected in a slowly rotating drum by recording them visually or by picking up with a microphone the characteristic noise made by tumbling beads and feeding this signal to a computer (*73*).

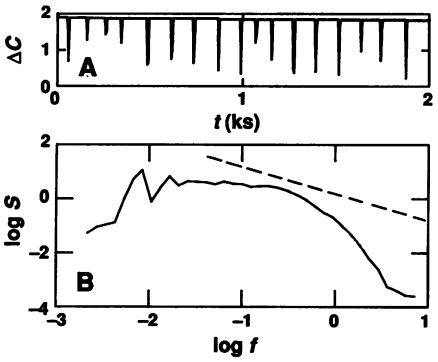

Fig. 6. (**A**) Time sequence of avalanches measured in the slowly rotating drum experiment of Fig. 5C. Sand falling out of the drum changes the capacitance (in arbitrary units) of a pair of capacitor plates through which it flows. Each spike corresponds to a global avalanche. There is a well-defined interval between successive events. (**B**) The power spectrum of the signal in (A) shows no evidence of power law behavior (S normalized to arbitrary units; f normalized to s^{-1}). The dashed line indicates how a $1/f$ power spectrum would have appeared. Each large spike in the signal corresponds to an avalanche that spans the entire system and consists of hundreds or even thousands of particles, depending on the system size. Each avalanche occurs after a well-defined interval of time has elapsed since the preceding event. The avalanches start at a maximally stable angle θ_m and return the pile to the (lower) angle of repose θ_r. The experiments show that there were practically no avalanches that were local and that did not span the entire system. The nearly uniform spacing of avalanches, $\langle\Delta t\rangle$, corresponds to the broadened peak at $f = 1/\langle\Delta t\rangle$ in the power spectrum shown in (B). The roll-off at high frequencies, above $f = 1/\langle\tau\rangle$, is due to the finite width τ of the individual avalanches. In the relevant frequency range, between $1/\langle\Delta t\rangle$ and $1/\langle\tau\rangle$, the spectrum appears to be approximately independent of frequency.

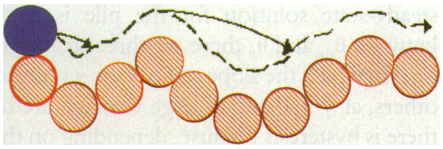

Fig. 7. Path of a particle following the terrain below it at a low shear rate (dashed line). At higher shear rate (solid line) it partially leaves the underlying surface.

corresponding to a finite shear rate $\dot{\gamma}$ in the sandpile.

Conversely, grain flow in an avalanche can be thought of as analogous to the onset of electrical current flow. In experiments of Clauss *et al.* (*82*) the nonlinear circuit element was a piece of slightly *p*-doped germanium at liquid helium temperatures. For voltage bias above a threshold, autocatalytic impact ionization, once started, builds up free-carrier avalanches that give rise to a current flow. The system oscillates in a regular manner just as shown in Fig. 6; each spike corresponds to a major breakdown event. Just below threshold, on the other hand, this semiconductor system exhibits a power law distribution of intervals between spikes that has been interpreted as self-organized critical behavior.

Conclusions

Much of the dynamical behavior found in granular material has analogs in other systems. We have mentioned some of these cases, such as the logarithmic decays found in spin glasses, ferrofluids, and superconductors. In addition, within the context of self-organized criticality, avalanches have been viewed as analogous to earthquakes (*83*). To describe fault instabilities, slip-weakening models have been introduced (*84*), which, as a function of slip velocity, exhibit negative differential friction as found in the model described above. Recent simulations of plate dynamics have been based on such force laws (*85*). Although initially thought to describe earthquake dynamics, they may actually be better suited for describing the avalanches in a sandpile (*86*). On a more microscopic scale, connections have been found between avalanche dynamics and grain-boundary formation or collapse in magnetic materials (*87*). Hysteresis in spin glasses was shown (*88, 89*) to correspond directly to mechanical hysteresis in a sandpile.

In this article we have emphasized fluctuations, noise, and instabilities to which a new and different kind of statistical theory may be relevant. Some of the problems we have mentioned have been around since the time of Faraday, such as the cause of the convection that is driven by large-scale vibrations. Others, such as the relation of the dynamics of avalanches to the predictions of self-organized critical behavior, are of more recent origin. Some questions are of immediate practical and technological importance, such as the behavior of flow through orifices and the dynamics of avalanches. Others, such as the mechanisms for wavelength selection in pattern formation, are currently of primarily scientific interest.

REFERENCES AND NOTES

1. S. B. Savage, *Adv. Appl. Mech.* **24**, 289 (1984).
2. R. M. Nedderman, U. Tüzün, S. B. Savage, G. T. Houlsby, *Chem. Eng. Sci.* **37**, 1597 (1982).
3. C. S. Campbell, *Annu. Rev. Fluid Mech.* **22**, 57 (1990).
4. See, for example, F. S. Vandervoort, *Sci. Teach.* **56**, 52 (April 1989).
5. J. D. Bernal, *Proc. R. Inst. G.B.* **37**, 355 (1959); *Proc. R. Soc. London Ser. A* **280**, 299 (1964).
6. G. D. Scott, *Nature* **188**, 908 (1960); *ibid.* **194**, 956 (1962).
7. J. L. Finney, *Proc. R. Soc. London Ser. A* **319**, 479 (1970).
8. G. Y. Onoda and E. G. Liniger, *Phys. Rev. Lett.* **64**, 2727 (1990).
9. O. Reynolds, *Philos. Mag.* **20**, 469 (1885).
10. T. Wakabayashi, in *Proceedings of the 9th Japanese National Congress on Applied Mechanics*, 1959 (Science Council of Japan, Ueno Park, Tokyo, Japan, 1960), pp. 133–140.
11. M. Ammi, T. Travers, J. P. Troadec, *J. Phys. D* **20**, 424 (1987).
12. P. A. Cundall, A. Drescher, O. D. L. Strack, in *Proceedings of the IUTAM Conference on Deformation and Failure of Granular Materials* (Delft, The Netherlands, 1982), pp. 355–370.
13. C. E. D. Ouwerkerk, in *Powder Technol.* **65**, 125 (1991).
14. E. Guyon *et al.*, *Rep. Prog. Phys.* **53**, 373 (1990).
15. P. M. Duxbury, P. D. Beale, P. L. Leath, *Phys. Rev. Lett.* **57**, 1052 (1986); P. M. Duxbury, P. L. Leath, P. D. Beale, *Phys. Rev. B* **36**, 367 (1987).
16. S. Ogawa, in *Proceedings of the U.S.–Japan Seminar on Continuum Mechanics and Statistical Approaches in Mechanics of Granular Materials* (Gukujutsu Bunken Fukyu-kai, Tokyo, 1978), p. 208.
17. H. M. Jaeger, C.-h. Liu, S. R. Nagel, *Phys. Rev. Lett.* **62**, 40 (1989).
18. S. F. Edwards, in *Proceedings of the International School of Physics: Enrico Fermi*, Course 106, G. F. Chiarotti, F. Fumi, M. P. Tosi, Eds. (North-Holland, New York, 1990), pp. 849–857; _____ and A. Mehta, *J. Phys.* (*Paris*) **50**, 2489 (1989).
19. A. Mehta and S. F. Edwards, *Phys. A* **157**, 1091 (1989).
20. _____, *ibid.* **168**, 714 (1990).
21. R. J. Baxter, *Phys. Rev. Lett.* **26**, 832 (1971).
22. S. B. Savage, in *Developments in Engineering Mechanics*, A. P. S. Selvadurai, Ed. (Elsevier, Amsterdam, 1987), p. 347.
23. P. K. Haff and B. T. Werner, *Powder Technol.* **48**, 239 (1986).
24. A. Rosato, K. J. Strandburg, F. Prinz, R. H. Swendsen, *Phys. Rev. Lett.* **58**, 1038 (1987).
25. C.-h. Liu and S. R. Nagel, in preparation.
26. J. Duffy and R. D. Mindlin, *J. Appl. Mech.* **24**, 585 (1957).
27. K. L. Johnson, *Contact Mechanics* (Cambridge Univ. Press, Cambridge, 1985).
28. J. D. Goddard [*Proc. R. Soc. London Ser. A* **430**, 105 (1990)] has attempted to explain the discrepancies between the $P^{1/6}$ law and the velocities measured by Duffy and Mindlin.
29. S. Washburn and R. Webb, *Adv. Phys.* **35**, 375 (1986).
30. A. D. Stone, *Phys. Rev. Lett.* **54**, 2692 (1985); P. A. Lee and A. D. Stone, *ibid.* **55**, 1622 (1985); B. L. Al'tshuler, *JETP Lett.* **41**, 648 (1985).
31. C. N. Guy, *J. Phys. F* **8**, 1309 (1978).
32. G. Hadjipanayis, D. J. Sellmyer, B. Brandt, *Phys. Rev. B* **23**, 3349 (1981); G. Hadjipanayis and D. J. Sellmyer, *ibid.*, p. 3355.
33. W. Luo, S. R. Nagel, T. F. Rosenbaum, R. E. Rosensweig, *Phys. Rev. Lett.* **67**, 2721 (1991).
34. M. Tuominen, A. M. Goldman, M. L. Mecartney, *Phys. Rev. B* **37**, 548 (1988); C. W. Hagen and R. Griessen, *Phys. Rev. Lett.* **62**, 2857 (1989); C. Rossel, Y. Maeno, I. Morgenstern, *ibid.*, p. 681; A. Hamzic, L. Fruchter, I. A. Campbell, *Nature* **345**, 515 (1990); I. A. Campbell, L. Fruchter, R. Cabanel, *Phys. Rev. Lett.* **64**, 1561 (1990).
35. D. K. Lottis, R. M. White, E. D. Dahlberg, *Phys. Rev. Lett.* **67**, 362 (1991).
36. See the review by C. W. Hagen and R. Griessen, in *Studies of High Temperature Superconductors*, A. V. Narlikar, Ed. (Nova Science, New York, 1989), vol. III, pp. 159–195.
37. See M. Tinkham, *Introduction to Superconductivity* (McGraw-Hill, New York, 1975) and references therein.
38. This connection was first suggested by P. G. de Gennes [*Superconductivity of Metals and Alloys* (Benjamin, New York, 1966), p. 83].
39. T. A. Duke, G. C. Barker, A. Mehta, *Europhys. Lett.* **13**, 19 (1990).
40. P. Evesque and J. Rajchenbach, *Phys. Rev. Lett.* **62**, 44 (1989).
41. C. Laroche, S. Douady, S. Fauve, *J. Phys.* (*Paris*) **50**, 699 (1989).
42. M. Faraday, *Trans. R. Soc. London* **52**, 299 (1831).
43. S. Duady, S. Fauve, C. Laroche, *Europhys. Lett.* **8**, 621 (1989).
44. R. A. Bagnold, *Proc. R. Soc. London Ser. A* **225**, 49 (1954); *ibid.* **295**, 219 (1966).
45. G. Hagen, *Berlin Mon.ber. Akad. Wiss.*, p. 35 (1852).
46. S. B. Savage and D. J. Jeffrey, *J. Fluid Mech.* **110**, 255 (1981); C. K. K. Lun, S. B. Savage, D. J. Jeffrey, N. Chepurniy, *ibid.* **140**, 223 (1984); C. K. K. Lun and S. B. Savage, *J. Appl. Mech.* **54**, 47 (1987).
47. J. T. Jenkins and M. W. Richman, *J. Fluid Mech.* **171**, 53 (1986); J. T. Jenkins and S. B. Savage, *ibid.* **130**, 187 (1983).
48. P. K. Haff, *ibid.* **134**, 401 (1983).
49. C. S. Campbell and C. E. Brennen, in *Proceedings of the IUTAM Conference on Deformation and Failure of Granular Materials* (Delft, The Netherlands, 1982), p. 515; O. R. Walton and R. L. Braun, *Acta Mech.* **63**, 73 (1986); *J. Rheol.* **30**, 949 (1986).
50. H. Caram and D. C. Hong, *Phys. Rev. Lett.* **67**, 828 (1991).
51. For overviews see S. B. Savage, *J. Fluid Mech.* **92**, 53 (1979); T. G. Drake, *J. Geophys. Res.* **95**, 8681 (1990).
52. S. B. Savage and M. Sayed, *J. Fluid Mech.* **142**, 391 (1984); D. M. Hanes and D. L. Inman, *ibid.* **150**, 357 (1985).
53. An example of a nonmechanical loading force is an applied magnetic field in the case of shear flow in magnetic powders [K. Craig, R. H. Buckholz, G. Domoto, *Phys. Fluids* **30**, 1993 (1987)].
54. T. Takahashi, *Annu. Rev. Fluid Mech.* **13**, 57 (1981).
55. M. Shibata and C. C. Mei, *Acta Mech.* **63**, 179 (1986); D. M. Hanes, *ibid.*, p. 131.
56. This, of course, is what is responsible for making an hourglass such a useful instrument for measuring time. For a review of the dependence of the flow rate through an aperture on other parameters, such as its diameter, see (*2*).
57. R. L. Brown and P. G. W. Hawksley, *Fuel* **27**, 159 (1947).
58. G. C. Gardner, *Chem. Eng. Sci.* **21**, 261 (1966).
59. P. M. Blair-Fish and P. L. Bransby, *J. Eng. Ind.* **95**, 17 (1973); S. Lee, S. C. Cowin, J. S. Templeton, *Trans. Soc. Rheol.* **18**, 247 (1974).
60. G. W. Baxter, R. P. Behringer, T. Fagert, G. A. Johnson, *Phys. Rev. Lett.* **62**, 2825 (1989).
61. D. G. Schaeffer, *J. Differ. Equ.* **66**, 19 (1987); E. B. Pitman and D. G. Schaeffer,

Comm. Pure Appl. Math. **40**, 421 (1987).
62. R. Jackson, in *Theory of Dispersed Multiphase Flow*, R. E. Meyer, Ed. (Academic Press, New York, 1983), pp. 291–337.
63. Unfortunately, the evolution equations for plastic flow in a uniform medium are often ill-posed [D. G. Schaeffer and E. B. Pitman, *Comm. Pure Appl. Math.* **41**, 879 (1988)].
64. G. W. Baxter and R. P. Behringer, *Phys. Rev. A* **42**, 1017 (1990).
65. P. Bak, C. Tang, K. Wiesenfeld, *Phys. Rev. Lett.* **59**, 381 (1987); C. Tang and P. Bak, *ibid.* **60**, 2347 (1988); K. Wiesenfeld, C. Tang, P. Bak, *J. Stat. Phys.* **54**, 1441 (1989).
66. Y. Zhang, *Phys. Rev. Lett.* **63**, 470 (1989); B. McNamara and K. Wiesenfeld, *Phys. Rev. A* **41**, 1867 (1990); K. Wiesenfeld, J. Theiler, B. McNamara, *Phys. Rev. Lett.* **65**, 949 (1990); J. M. Carlson, J. T. Chayes, E. R. Grannan, G. H. Swindle, *ibid.*, p. 2548; *Phys. Rev. A* **42**, 2467 (1990); S. S. Manna, *J. Stat. Phys.* **59**, 509 (1990); P. Grassberger and S. S. Manna, *J. Phys.* (*Paris*) **51**, 1077 (1990); J. Honkonen, *Phys. Lett. A* **145**, 87 (1990).
67. K. P. O'Brien, L. Wu, S. R. Nagel, *Phys. Rev. A* **43**, 2052 (1991).
68. T. Hwa and M. Kardar, *Phys. Rev. Lett.* **62**, 1813 (1989).
69. L. P. Kadanoff, S. R. Nagel, L. Wu, S.-M. Zhou, *Phys. Rev. A* **39**, 6524 (1989).
70. T. C. Halsey, P. Meakin, I. Procaccia, *Phys. Rev. Lett.* **56**, 854 (1986); T. C. Halsey, M. H. Jensen, L. P. Kadanoff, I. Procaccia, B. I. Shraiman, *Phys. Rev. A* **33**, 1141 (1986).
71. D. Train, *J. Pharm. Pharmacol.* **10**, 127T (1958); N. Pilpel, *Chem. Process. Eng.* (*Bombay*) **46**, 167 (1965).
72. G. A. Held *et al.*, *Phys. Rev. Lett.* **65**, 1120 (1990).
73. P. Evesque and J. Rajchenbach, *C. R. Acad. Sci. Ser. II* (*Paris*) **307**, 223 (1988).
74. H. J. Jensen, K. Christiansen, and H. C. Fogedby [*Phys. Rev. B* **40**, 7425 (1989)] used the same model and showed that $\alpha = 2$ in both one and two dimensions.
75. C.-h. Liu, H. M. Jaeger, S. R. Nagel, *Phys. Rev. A* **43**, 7091 (1991).
76. P. Evesque and J. Rajchenbach, in *Powders and Grains*, J. Biarez and R. Gourves, Eds. (Balkema, Rotterdam, The Netherlands, 1989), p. 217; see also (*73*).
77. P. Evesque, *Phys. Rev. A* **43**, 2720 (1991).
78. H. M. Jaeger, C.-h. Liu, S. R. Nagel, T. A. Witten, *Europhys. Lett.* **11**, 619 (1990).
79. C.-A. de Coulomb, in *Mémoires de Mathématiques et de Physique Présentés à L'Académie Royale des Sciences par Divers Savans et Lus dans les Assemblées* (l'Imprimerie Royale, Paris, 1773), pp. 343–382.
80. K. H. Roscoe, *Geotechnique* **20**, 129 (1970); see also (*52*).
81. P. A. Thompson and G. S. Grest, *Phys. Rev. Lett.* **67**, 1751 (1991).
82. W. Clauss *et al.*, *Europhys. Lett.* **12**, 423 (1990).
83. A. Sornette and D. Sornette, *ibid.* **9**, 197 (1989); P. Bak and C. Tang, *J. Geophys. Res.* **94**, 15635 (1989).
84. See J. R. Rice, *Pure Appl. Geophys.* **121**, 443 (1983).
85. J. M. Carlson and J. S. Langer, *Phys. Rev. Lett.* **62**, 2632 (1989).
86. M. de Sousa Vieira, G. L. Vasconcelos, S. R. Nagel, in preparation.
87. K. L. Babcock and R. M. Westervelt, *Phys. Rev. Lett.* **64**, 2168 (1990).
88. J. Souletie, *J. Phys.* (*Paris*) **44**, 1095 (1983).
89. E. M. Gyorgy, R. B. van Dover, K. A. Jackson, L. F. Schneemeyer, J. V. Wasczak, *Appl. Phys. Lett.* **55**, 283 (1989).
90. We are grateful to T. C. Halsey and T. A. Witten for a critical reading of the manuscript and to R. Jeshion and J. Lemon for many helpful suggestions regarding its style. We also thank R. P. Behringer and G. W. Baxter for providing Figs. 2 and 3. C.-h. Liu, L. P. Kadanoff, K. P. O'Brien, T. A. Witten, L. Wu, and S.-M. Zhou collaborated on various aspects of the work. Supported by NSF grant DMR-MRL 88-19860.

Explosives Detection for Aviation Security

ANTHONY FAINBERG

The threat of terrorism against commercial aviation has received much attention in the past few years. In response, new ways to detect explosives and to combine techniques based on different phenomena into integrated security systems are being developed to improve aviation security. Several leading methods for explosives and weapons detection are presented.

IN THE PAST 20 YEARS, TERRORIST ATTACKS HAVE TAKEN ON AN increasingly international flavor, becoming acknowledged weapons in political and military disputes. As Clausewitz referred to war as being an extension of politics, so might terrorism be considered an extension of war, to be used when politics or war may not be as likely to accomplish the political goals of the practitioners. The advent of mass attacks on innocent individuals by means of car bombs, airline sabotage, and random mass attacks on passersby in public places has alarmed much of the world. Because of the shock at the spectacle of such events and because of the fear that all are vulnerable to this predation, there have been increasing calls on governments to do more to protect the public.

One way to counter terrorism is to satisfy the demands of the terrorists, especially when they advocate politically defensible or popular causes. However, capitulation or concessions are usually difficult to sustain politically and do not always resolve the problem. Another strategy for defense is to threaten and carry out military action against states that sponsor terrorism. The drawbacks of this strategy are that many acts of terrorism have no state sponsors and that many innocent people, residents of the targeted state, may be killed or wounded by such actions, even if the actions are carefully directed at military targets. Yet another way of defending the public is for authorities to infiltrate terrorist groups to gain advance notice of attacks, enabling them to forestall planned operations. This technique is frequently utilized by intelligence services around the world. It is often successful, although successes do not always come to the attention of the public. Infiltration and intelligence gathering do not, however, always work; there will always be some attacks that cannot be prevented by such means.

This article discusses some options for combating a major type of terrorism, airline bombings, in a fourth way: through the use of technology. This is a field in which the targets, often advanced Western states, may have a decided advantage over the terrorists. There is clearly no technical "fix" for such attacks. However, technology is a tool that can be used in conjunction with others to help reduce the frequency of terrorist acts, to mitigate such acts when they occur, and thereby to help save the lives of countless innocent victims. It is a tool that has been underrated in the past: research and development in relevant areas has not been funded particularly well—about $70 million in federal appropriations have been identified for fiscal year 1990, less than 1% of total Department of Defense appropriations for similar levels of research and development.

Although domestic terrorism in the United States has been minimal in the last few years, American targets have been the objects of a large fraction of international terrorist incidents. Following the Gulf War, fears grew that Iraqi agents or their sympathizers would unleash terror against U.S. citizens around the world. Fortunately, these fears were not realized, but there still is concern that such attacks could occur in the near future. To understand how technol-

The author is at the Center for International Security and Arms Control at Stanford University, Stanford, CA 94305, on leave from the Office of Technology Assessment, U.S. Congress, Washington, DC 20510.